Chemosphere 153 (2016) 287–293

Contents lists available at ScienceDirect

Chemosphere

journal homepage: www.elsevier.com/locate/chemosphere

Effects of chlorpyrifos on the gut microbiome and urine metabolome in mouse (*Mus musculus*)

Yanping Zhao [a], Yan Zhang [b], Guoxiang Wang [a, *], Ruiming Han [a], Xianchuan Xie [c]

[a] Jiangsu Key Laboratory of Environmental Change and Ecological Construction, Jiangsu Center for Collaborative Innovation in Geographical Information Resource Development and Application, School of Geographical Science, Nanjing Normal University, Nanjing 210023, China
[b] State Key Laboratory of Pollution Control and Resource Reuse, School of the Environment, Nanjing University, Nanjing 210023, China
[c] State Key Laboratory of Pollution Control and Resource Reuse, Center for Hydrosciences Research, School of the Environment, Nanjing University, Nanjing 210023, China

HIGHLIGHTS

- Toxic effects of CPF on mice gut microbiome and urine metabolome were investigated.
- CPF changed the gut microbiota composition and metabolism related genes expression.
- Some gut microbiota-related metabolites were perturbed by CPF exposure.

GRAPHICAL ABSTRACT

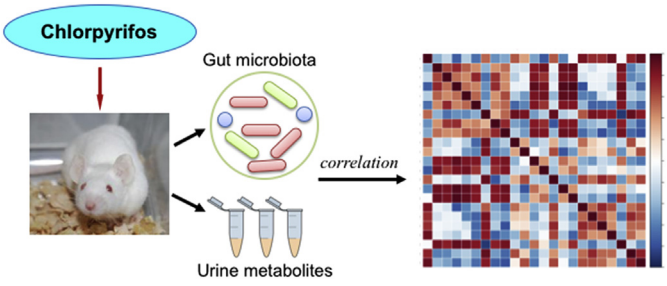

ARTICLE INFO

Article history:
Received 5 November 2015
Received in revised form
10 March 2016
Accepted 13 March 2016

Handling Editor: A. Gies

Keywords:
Chlorpyrifos
High-throughput sequencing
Metabolomics
Gut microbiome
Mice

ABSTRACT

In this study, the toxic effects of clorpyrifos (CPF) on the gut microbiome and related urine metabolome in mouse (*Mus musculus*) were investigated. Mice were exposed to a daily dose of 1 mg kg^{-1} bodyweight of CPF for 30 d. As a result, CPF significantly altered the gut microbiota composition in terms of the relative abundance of key microbes. Meanwhile, CPF exposure induced the alterations of urine metabolites related to the metabolism of amino acids, energy, short-chain fatty acids (SCFAs), phenyl derivatives and bile acids. High correlations were observed between perturbed gut microbiome and altered metabolic profiles. These perturbations finally resulted in intestinal inflammation and abnormal intestinal permeability, which were also confirm by the histologic changes in colon and remarkable increase of lipopolysaccharide (LPS) and diamine oxidase (DAO) in the serum of CPF-treated mice. Our findings will provide a new perspective to reveal the mechanism of CPF toxicity.

1. Introduction

Clorpyrifos (CPF), an organothiophosphate pesticide, has been banned in homes but still commonly used on farms (Giesy et al., 2014). CPF residues are often detected in food and drinking water (Bolles et al., 1999). The oral route is the major route of exposure for

* Corresponding author. 1, Wenyuan Road, Xianlin University District, Nanjing 210023, China.
E-mail address: wangguoxiang@njnu.edu.cn (G. Wang).

http://dx.doi.org/10.1016/j.chemosphere.2016.03.055
0045-6535/

the general population. It has been reported that the average dose ingested by an individual is about 1 mg d^{-1} (Joly et al., 2013). The neurotoxicity of CPF is of worldwide concern and acetylcholinesterase (AChE) inhibition is the principal mechanism (Chanda et al., 1996). Considering the oral route for human exposure, many studies began to focus on the impact of CPF on intestinal barrier and gut microbiome. It has been demonstrated that CPF could increase the intestinal permeability in rat (Cook and Shenoy, 2003; Tirelli et al., 2007; Condette et al., 2014). Chronic exposure to low dose of CPF induced dysbiosis in the microbial community (Joly et al., 2013; Xia et al., 2013).

Gut microbiome refers to trillions of microorganisms residing in the intestine and has a mutualistic relationship with its host (Bäckhed et al., 2005). Gut microbiome plays an important role to keep host health, enhance the immune system and regulate host metabolism (Turnbaugh et al., 2006; Tremaroli and Backhed, 2012). Nicholson et al. (2012) define a host-microbe metabolic axis as a multidirectional interactive chemical communication highway between specific host cellular pathways and a series of microbial species, subecologies, and activities. For example, bile acids, choline, and short-chain fatty acids (SCFAs) are produced by gut microbes, and the production of these metabolites contributes to the host metabolic phenotype and hence to disease risk.

The composition of the core gut microbiota is relatively stable. However, there are components that are dynamic and biologically and metabolically flexible, responding to perturbations of environmental stresses (Clemente et al., 2012). Emerging evidences have linked changes in the gut microbiome with the influence of environmental chemicals, such as polychlorinated biphenyls (PCBs) (Choi et al., 2013), environmental endocrine disruptors (EEDs) (Al-Asmakh et al., 2014), and heavy metals (Breton et al., 2013). Conversely, studies have shown that gut microbiota could modulate the detoxification of environmental chemicals by influencing the level and activity of host phase I and II enzymes, enterohepatic circulation, and gut barrier function (Snedeker and Hay, 2012). In this context, assessing the correlation between toxic effects of environmental toxins and alterations of gut microbiome is of great significance.

Metabolomics has been demonstrated to be valuable for revealing the mechanisms of toxicity (Robertson et al., 2011). Alterations of metabolic profiles are also known to be sensitive to external environmental stimulus, since relative subtle changes in metabolome can be detected in response to environmental chemicals exposure. Metabolomics studies have been conducted to evaluate the toxicity of CPF (Wang et al., 2009; Baylay et al., 2012; Kokushi et al., 2015). However, little is known about the gut microbiome - related metabolic changes associated with the CPF - altered gut microbiota community.

In this study, we used high-throughput sequencing and nuclear magnetic resonance (NMR) based metabolomics together to investigate the toxic effects of CPF on the gut microbiome and urine metabolome in mice. In addition, histopathology and intestinal permeability measurement were also used to detect the adverse effects of CPF on intestinal function.

2. Materials and methods

2.1. Animal treatment

Male mice (*Mus musculus* KM, ten-week-old) were purchased from experimental animal center of Academy of Military Medical Science of China. After two weeks acclimation, all mice were randomly divided into two groups: the control group (n = 5, treated with a corn oil vehicle by gavage once daily) and CPF-treat group (n = 5, treated with 1 mg CPF kg^{-1} bodyweight in corn oil vehicle once daily for 30 d). Mice were maintained in a 12/12 h light/dark cycle at 25 ± 3 °C, 50 ± 5% relative humidity, with free access to standard mouse chow (purchased from JSXTSW Co., Ltd., Nanjing of China, and the chemical composition is provided in the Supporting Information Table S1) and water. All experimental processes were in accordance with NIH Guide for the Care and Use of Laboratory animals. And the protocol was approved by the Committee on the Ethics of Animal Experiments of the Nanjing Military General Hospital.

CPF was purchased from Sigma-Aldrich. The CPF exposure dose employed was chosen based on previous reports that the average dose daily ingested by per person (Joly et al., 2013). After exposed to CPF for 30 days, all mice were euthanized with diethyl ether. Urine and fecal samples were collected using metabolic cages for 12 h before necropsy. Serum samples were collected during necropsy. Parts of intestine were dissected and fixed in formalin solution.

2.2. Histopathological analysis

The intestine samples of mice from control and CPF treated group were fixed in formalin, embedded in paraffin, sectioned at 4 μm, and stained with hematoxylin-eosin (H&E) for microscopic observation (7 tissue samples for each group and 5 slices for each tissue).

2.3. Intestinal permeability analysis

Serum lipopolysaccharide (LPS) and diamine oxidase (DAO) are useful markers to assess the intestinal injury and to monitor the increase of intestinal permeability (Hartmann et al., 2012; Hilsden et al., 1999). In this study, LPS and DAO levels in serum were measured by using LPS ELISA Kit and DAO Assay Kit (Jiancheng, Bioeng. Inst., China), respectively. Each assay was run in triplicate.

2.4. Illumina high-throughput sequencing

Total DNA was isolated from fecal samples by using FastDNA SPIN Kit for Soil (MP Biomedicals, CA, USA). After being quantified, the DNA samples were barcoded, pooled to construct the sequencing library and then were sequenced on a Hiseq 2500 platform (Illumina, USA) with paired end sequencing strategy. Equal amount of sequencing reads was generated for each sample. The process of quality control and raw data filtration refer to previous studies (Zhang et al., 2015).

2.5. Taxonomic classification

The filtered reads were uploaded and analyzed by MG-RAST (http://metagenomics.anl.gov/) with accession numbers of 232423, 232586, 232592, 232606, 232694, 232736, 232757, 239265, 239328 and 235581. Moreover, Metagenomic Phylogenetic Analysis (MetaPhlAn) (http://huttenhower.sph.harvard.edu/galaxy) was used for taxonomic classification. For higher confidence in the assignment, all analysis was conducted at the family level.

2.6. Metabolomic profiling

^{1}H NMR spectra of urine samples were acquired using a Bruker AV600 spectrometer (Bruker Co., Germany) at 298 K and 600.13 MHz, as demonstrated previously (Zhang et al., 2012). Metabolomics profiling data were processed as described previously (Deng et al., 2014). Partial least squares-discriminate analysis (PLS-DA) for the spectra data was performed on MetaboAnalyst 3.0. The metabolite resonances were identified according to Human

Metabolome Database (Deng et al., 2014). Significantly changed metabolites were identified based on the following criteria: fold change >1.20 and $p < 0.05$.

2.7. Statistical analysis

Relative abundance of each taxonomic group was calculated by dividing the read count of identified sequences by the total read count in individuals. A 100% stacked column chart comparing the relative abundances of each phylum in the two groups was generated using Microsoft Excel. Principal coordinate analysis (PCoA) was used to compare the gut microbiome profiles between control and treatment groups. In addition, hierarchical clustering analysis via the unweighted pair group method with arithmetic mean (UPGMA) was conducted to assess the difference in the gut microbiome composition. The correlation matrix between the gut microbes and altered urine metabolites was generated using Pearson's correlation coefficient and visualized by using R. The Benjamini-Hochberg method was used for FDR control (FDR < 0.05). Mann-Whitney test was used to evaluate the statistical differences of biological parameters between control and treatment groups. $P < 0.05$ was accepted as significance.

3. Results

3.1. Histopathological changes and intestinal injury induced by CPF

H&E stained histopathological sections of colon were analyzed under a microscope and the representative sections are shown in Fig. 1A and B. The average percentages of adverse histological changes were calculated and the results were listed in Table S2. Compared with control group, intestinal epithelial edema (79%), inflammation (81%), and necrosis (80%) were observed in CPF-treated group. In addition, LPS and DAO levels in serum were also detected to assess the intestinal injury. Fig. 1C and D illustrate that CPF exposure resulted in significantly increased LPS and DAO in serum from CPF-treated mice.

3.2. Gut microbiome changes induced by CPF

In this study high-throughput sequencing was used to detect the changes of gut microbiota community in mice due to CPF exposure. The identified gut bacteria assigned at the phylum level from 16S rRNA sequencing reads is shown in Fig. 2A. As a result, the gut microbiota in control and CPF-treated mice were all dominated by *Firmicutes* (32%–66%), *Bacteroidetes* (18%–42%), and *Proteobacteria* (6%–21%).

Multivariate statistical analysis-PCoA was used to reveal the difference in the gut microbiome patterns in response to CPF exposure. As a result, CPF induced significant differences in the gut microbiome, as shown by the PCoA plot in Fig. 2B. CPF-treated mice are clearly separated from control mice, with 65.95% and 12.35% variation explained by PC1 and PC2, respectively. Meanwhile, hierarchical clustering analysis with UPGMA was conducted and the results were consistent with the PCoA plot, that all control and CPF-treated mice successfully clustered in their own groups (Fig. 2C).

These differences of gut microbiome patterns can be directly attributed to the changes of relative abundance of dominant gut bacteria. For the most predominant phyla, the relative abundance of *Firmicutes* was significantly decreased in treated mice, while that of *Bacteroidetes* was significantly elevated (Fig. 2D). Furthermore, among the dominant families, the relative abundance of

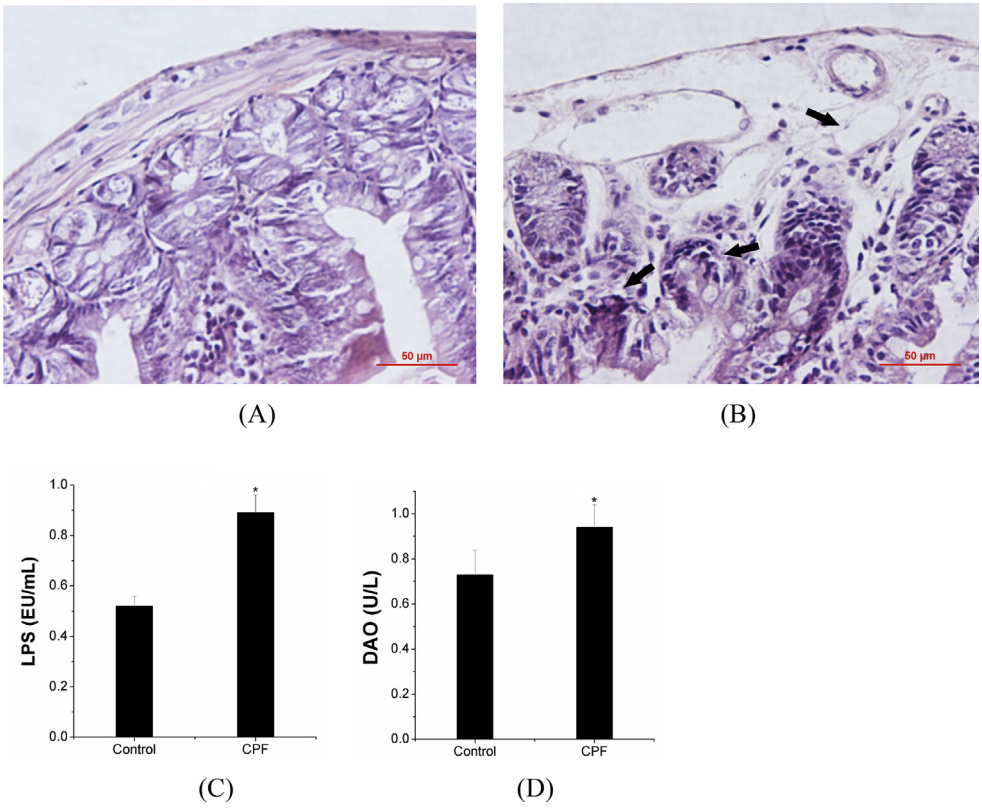

Fig. 1. Representative images of H&E-stained colon sections of intestine from mice in the control (A) and CPF-treated group (B). LPS level (C) and DAO level (D) in mice serum under CPF exposure. Black arrows indicate histological changes. Bars represent standard deviation of the mean, $^{*}p < 0.05$.

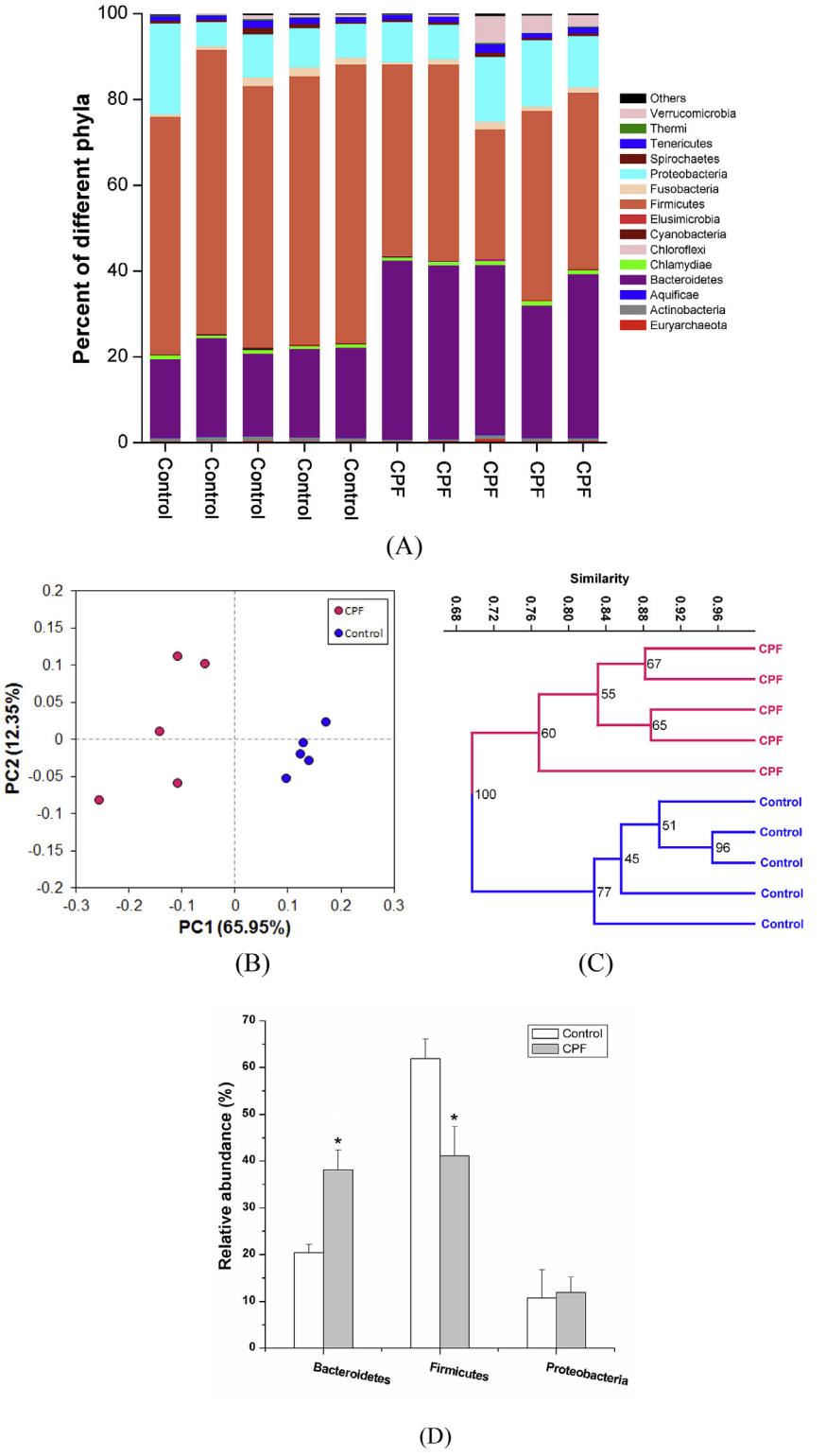

Fig. 2. (A) The gut microbiome composition individual profiles at the phylum level in the control and CPF-treated mice. (B) Principal coordinate analysis for the gut microbiome patterns of control and CPF-treated mice. The percentage of variation explained by the plotted principal coordinates is indicated on the axes. (C) Hierarchical clustering analysis by UPGMA. (D) Relative abundance of predominant phyla in gut bacteria from control and CPF-treated mice. $^{*}p < 0.05$.

Lactobacillaceae was significantly decreased while the relative abundance of *Bacteroidaceae* was significantly increased under CPF exposure (Table S3).

3.3. CPF-induced changes in urine metabolic profiles

In this study, ^{1}H NMR based metabolomics was used to determine the alterations of metabolic profiles in mice urine in response

to CPF exposure. PLS-DA model was conducted on the NMR data sets of all individuals and the first two primary components PC1 and PC2 were selected to identify the discrimination between CPF-treated and control mice. As a result, the control and CPF-treated groups were successfully separated, with 5.1% and 75.9% variation explained by PC1 and PC2, respectively (Fig. 3).

In addition, compared with control group, a total of 24 metabolites were significantly changed (fold change >1.20 and $p < 0.05$) in the CPF-treated group, and 7 metabolites were increased and 17 metabolites were decreased (Table S4). These metabolites related to different metabolism pathways, such as amino acid metabolism (glutamate, leucine, lysine, threonine, and tyrosine), energy metabolism (acetone, creatine, fumarate, glucose and glycerol), SCFAs metabolism (hexanoate, isobutyrate, isovalerate and valerate), phenyl derivatives metabolism (phenylacetylglycine, phenylalanine and phenylpropionylglycine), indole derivatives metabolism (indoleacetate), bile acids metabolism (deoxycholate, lithocholate and taurocholate), polyamines metabolism (cadaverine), and vitamins metabolism (biotin and pyridoxine). While, acetate and butyrate, as the main SCFAs, did not changed with the treatment.

3.4. Correlation between the gut microbiome and host metabolites

Pearson's correlation coefficient was calculated to identify the correlations between perturbed gut microbiota and altered urine metabolites (Fig. 4). As a result, clear correlations between specific gut bacteria and urine metabolites were found. For example, *Bifidobacteriaceae* was positively correlated with glycerol, phenylacetylglycine, and lithocholate. *Bacteroidaceae*, *Sphingobacteriaceae*, *Erysipelotrichaceae*, *Halobacteroidaceae*, *Lactobacillaceae*, and *Enterobacteriaceae* were highly correlated with amino acid, energy and phenyl derivatives related metabolites. In addition, *Lactobacillaceae* was also positively correlated with SCFAs-related metabolites (hexanoate and valerate).

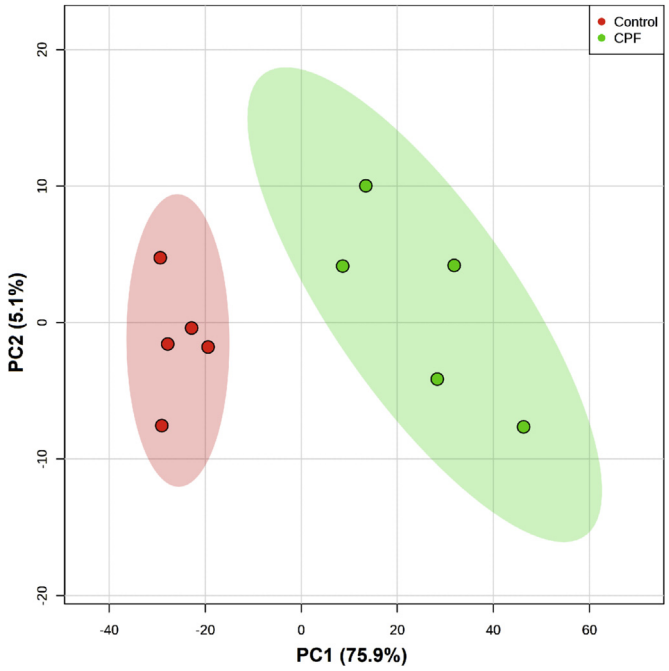

Fig. 3. Scatter plot of PLS-DA for metabolic profiles.

4. Discussion

In this study, histopathological examination and ELISA were used to determine the intestinal lesions induced by CPF exposure. Intestinal epithelial cells play critical roles in regulation of barrier function and immune homeostasis. Intestinal epithelial inflammation was observed in CPF-treated mice, indicating intestinal injury induced by CPF exposure. LPS is also termed endotoxin and used as a marker of bacterial tissue invasion and inflammation (Rosenfeld and Shai, 2006). DAO is an intracellular enzyme with high activity and can be used as a sensitive maker to determine mucosal barrier function (Sun et al., 2013). The increased serum LPS and DAO in CPF-treated mice indicated that CPF exposure induced significant inflammation and increase of intestinal permeability. Cook and Shenoy (2003) have demonstrated that CPF exposure could induce inflammatory responses and increase intestinal permeability in rats. Tirelli et al. (2007) found that CPF could result in impairment of barrier integrity of intestine in vitro model. Abnormal intestinal permeability could be induced by many environmental risk factors and trigger various diseases, such as inflammatory bowel diseases (IBD) (Danese et al., 2004).

Intestinal inflammation has strong associations with gut microbiota (Maslowski et al., 2009). It has been demonstrated that the gut microbiota of human and mice are dominated by two major phyla, *Firmicutes* and *Bacteroidetes* (Sommer and Backhed, 2013; Nguyen et al., 2015). However, when exploring deeper taxonomic classifications, most bacterial genera (85%) in mouse gut are not present in human (Ley et al., 2005). In this study, microbiota composition of was unstable at the phylum level with an increase in *Bacteroidetes* at the expense of *Firmicutes* in the CPF-treated mice. Such shifts of *Firmicutes* and *Bacteroidetes* were previously shown to be significantly correlated with chronic intestinal inflammation (Walker et al., 2011). Similar results have been demonstrated in the Simulator of the Human Intestinal Microbial Ecosystem (SHIME) and in rats that low-dose exposure to CPF could induce dysbiosis in the microbial community (Joly et al., 2013). These results suggested that CPF exposure induced perturbations in the gut microbiota with regard to the relative abundance of specific microbial communities.

In this study, metabolomic profiling was used to investigate the impact of CPF on mice urine metabolic profiles. As a result, amino acids and energy related metabolites were significantly changed. As previous metabolomics studies have also demonstrated that exposure to CPF could cause disturbance in amino acid and energy metabolism in rats (Xu et al., 2015), fish (Kokushi et al., 2015), and earthworm (Baylay et al., 2012). In addition, in our study, *Bacteroidetes* (*Bacteroidaceae*, *Porphyromonadaceae*, and *Sphingobacteriaceae*) and *Firmicutes* (*Erysipelotrichaceae*, *Halobacteroidaceae*, *Lactobacillaceae*) were highly correlated with amino acid and energy related metabolites here. Gut microbiota may have a pivotal role in the maintenance of amino acid and energy homeostasis in rodent and human (Musso et al., 2010; Nicholson et al., 2012). These results suggested that CPF exposure induced disruptions of amino acid and energy metabolism in mice and these metabolic alterations have functional correlation with the gut microbiota.

Furthermore, some metabolites of SCFAs, phenyl derivatives and bile acids were also significantly changed. The metabolism of SFCAs, bile acids, and phenyl derivatives are essential for host health and the production of these metabolites by gut microbes may influence the host metabolic phenotype or disease risk. Alterations of these metabolites were previously reported as a consequence of perturbation in gut microbiota (Nicholson et al., 2012).

SCFAs are one of the most important gut microbial products and affect the energy utilization of host (den Besten et al., 2013). It has been demonstrated that Clostridial clusters IV and XIVa of

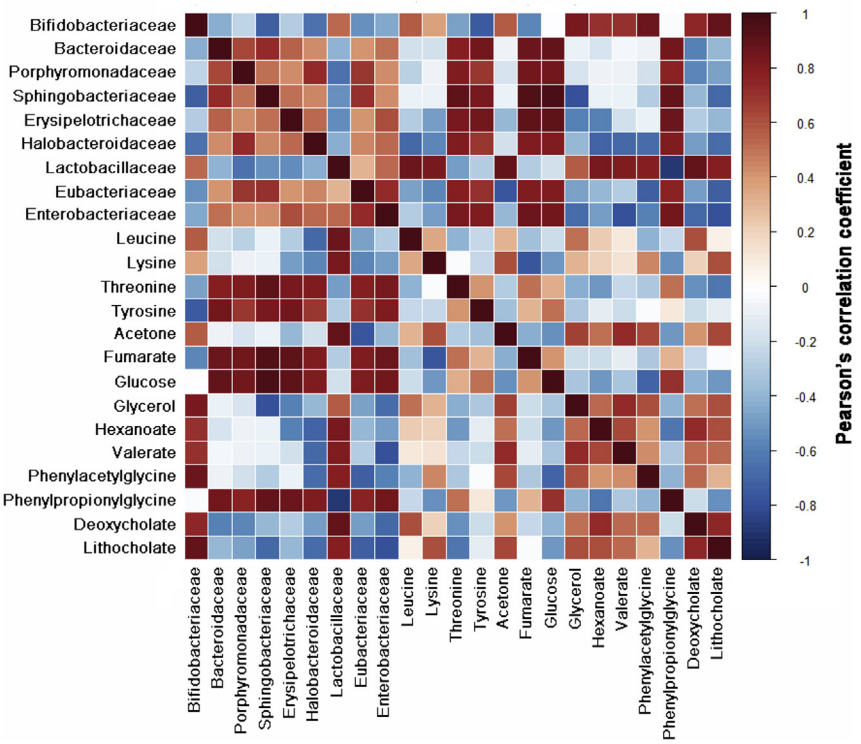

Fig. 4. Correlation plot showing the correlations between perturbed gut bacteria families and altered urine metabolites.

Firmicutes, including species of *Eubacterium*, *Roseburia*, *Faecalibacterium*, and *Coprococcus* are all related to SCFA metabolism in host (Scheppach, 1994; Wong et al., 2006). In this study, hexanoate and valerate had positive correlation with *Lactobacillaceae*. In addition, perturbations in energy metabolism were observed based on alterations of related metabolites.

The production of phenyl derivatives in mammals has been attributed to various genera of *Clostridum*, *Bifidobacterium*, *Subdoligramulum*, and *Lactobacillus* (Lord and Bralley, 2008; Zheng et al., 2011). In this study, the phenyl derivatives of phenylacetylglycine had positive correlation with *Bifidobacteriaceae*, while phenylpropionylglycine had negative correlation with *Lactobacillaceae*. The abundance of *Lactobacillaceae* was significantly decreased under CPF exposure. This condition is similar with the case of IBD (Ott and Schreiber, 2006). Correspondingly, intestinal injury was found in the CPF-treated mice.

About 5–10% of bile acids are biotransformed largely through degradation by gut bacteria, such as the genera of *Bacteroids*, *Enterobacter*, *Clostridum*, *Lactobacillus*, and *Bifidobacteria* (Nicholson et al., 2012). In this study, the bile acids such as deoxycholate and lithocholate only had positive correlation with the families of *Lactobacillaceae* and *Bifidobacteriaceae*, respectively. It indicated that CPF exposure induced alterations of specific gut bacteria related to bile acids metabolism. Since bile acids are essential for the metabolism of lipid and play an important role to maintain intestinal barrier function and regulate energy homeostasis (Ogata et al., 2003; Lefebvre et al., 2009). Correspondingly, abnormal intestinal permeability and perturbed energy metabolism were induced due to CPF exposure.

5. Conclusion

In this study, significant perturbations in relative abundance of gut microbiota in mice were induced by CPF exposure. Meanwhile, CPF exposure also induced significantly changed urine metabolites, which are related to the metabolism of amino acids, energy, SCFAs, phenyl derivatives and bile acids. Moreover, these altered metabolites were highly correlated with specific gut microbiota families. These results suggested that CPF induced changes in intestinal bacterial community structure and disturbed the metabolic functions of gut microbiome. These perturbations finally resulted in intestinal inflammation and abnormal intestinal permeability. Our findings may provide novel insights into the mechanism of CPF or other environmental chemicals induced health risk.

Acknowledgements

This work was financially supported by the National Natural Science Foundation of China (No. 21407076, No. 21507058, No. 41203062), the Jiangsu Taihu Lake Water Environment Management Research (No. TH2014402), the Natural Science Foundation of Jiangsu Province (BK20130559) and the National Key Technology Support Program (2014BAC08B07).

Appendix A. Supplementary data

Supplementary data related to this article can be found at http://dx.doi.org/10.1016/j.chemosphere.2016.03.055.

References

Al-Asmakh, M., Stukenborg, J.-B., Reda, A., Anuar, F., Strand, M.-L., Hedin, L., Pettersson, S., Soeder, O., 2014. The gut microbiota and developmental programming of the testis in mice. PLoS One 9, e103809.

Bäckhed, F., Ley, R.E., Sonnenburg, J.L., Peterson, D.A., Gordon, J.I., 2005. Host-bacterial mutualism in the human intestine. Science. 307, 1915–1920.

Baylay, A.J., Spurgeon, D.J., Svendsen, C., Griffin, J.L., Swain, S.C., Sturzenbaum, S.R., Jones, O.A.H., 2012. A metabolomics based test of independent action and concentration addition using the earthworm *Lumbricus rubellus*. Ecotoxicology 21, 1436–1447.

Bolles, H.G., Dixon-White, H.E., Peterson, R.K., Tomerlin, J.R., Day, E.W.,

Oliver Jr., G.R., 1999. U.S. Market Basket study to determine residues of the insecticide chlorpyrifos. J. Agric. Food Chem. 47, 1817–1822.
Breton, J., Daniel, C., Dewulf, J., Pothion, S., Froux, N., Sauty, M., Thomas, P., Pot, B., Foligne, B., 2013. Gut microbiota limits heavy metals burden caused by chronic oral exposure. Toxicol. Lett. 222, 132–138.
Chanda, S.M., Pope, C.N., 1996. Neurochemical and neurobehavioral effects of repeated gestational exposure to chlorpyrifos in maternal and developing rats. Pharmacol. Biochem. Behav. 53, 771–776.
Choi, J.J., Eum, S.Y., Rampersaud, E., Daunert, S., Abreu, M.T., Toborek, M., 2013. Exercise attenuates PCB-induced changes in the mouse gut microbiome. Environ. Health Perspect. 121, 725–730.
Clemente, J.C., Ursell, L.K., Parfrey, L.W., Knight, R., 2012. The impact of the gut microbiota on human health: an integrative view. Cell 148, 1258–1270.
Condette, C.J., Khorsi-Cauet, H., Morliere, P., Zabijak, L., Reygner, J., Bach, V., Gay-Queheillard, J., 2014. Increased gut permeability and bacterial translocation after chronic chlorpyrifos exposure in rats. PLoS One 9, e102217.
Cook, T.J., Shenoy, S.S., 2003. Intestinal permeability of chlorpyrifos using the single-pass intestinal perfusion method in the rat. Toxicology 184, 125–133.
Danese, S., Sans, M., Fiocchi, C., 2004. Inflammatory bowel disease: the role of environmental factors. Autoimmun. Rev. 3, 394–400.
den Besten, G., van Eunen, K., Groen, A.K., Venema, K., Reijngoud, D.J., Bakker, B.M., 2013. The role of short-chain fatty acids in the interplay between diet, gut microbiota, and host energy metabolism. J. Lipid Res. 54, 2325–2340.
Deng, Y.F., Zhang, Y., Zhang, R., Wu, B., Ding, L.L., Xu, K., Ren, H.Q., 2014. Mice in vivo toxicity studies for monohaloacetamides emerging disinfection byproducts based on metabolomic methods. Environ. Sci. Technol. 48, 8212–8218.
Giesy, J.P., Solomon, K.R., Cutler, G.C., Giddings, J.M., Mackay, D., Moore, D.R.J., Purdy, J., Williams, W.M., 2014. Ecological risk assessment of the uses of the organophosphorus insecticide chlorpyrifos, in the United States. In: Giesy, J.P., Solomon, K.R. (Eds.), Ecological Risk Assessment for Chlorpyrifos in Terrestrial and Aquatic Systems in the United States. Springer Int Publishing Ag, Cham, pp. 1–11.
Hartmann, P., Haimerl, M., Mazagova, M., Brenner, D.A., Schnabl, B., 2012. Toll-like receptor 2-mediated intestinal injury and enteric tumor necrosis factor receptor I contribute to liver fibrosis in mice. Gastroenterology 143, 1330–1340.
Hilsden, R.J., Meddings, J.B., Hardin, J., Gall, D.G., Sutherland, L.R., 1999. Intestinal permeability and postheparin plasma diamine oxidase activity in the prediction of Crohn's disease relapse. Inflamm. Bowel Dis. 5, 85–91.
Joly, C., Gay-Queheillard, J., Leke, A., Chardon, K., Delanaud, S., Bach, V., Khorsi-Cauet, H., 2013. Impact of chronic exposure to low doses of chlorpyrifos on the intestinal microbiota in the Simulator of the Human Intestinal Microbial Ecosystem (SHIME (R)) and in the rat. Environ. Sci. Pollut. Res. 20, 2726–2734.
Kokushi, E., Uno, S., Pal, S., Koyama, J., 2015. Effects of chlorpyrifos on the metabolome of the freshwater carp. Cyprinus Carpio. Environ. Toxicol. 30, 253–260.
Lefebvre, P., Cariou, B., Lien, F., Kuipers, F., Staels, B., 2009. Role of bile acids and bile acid receptors in metabolic regulation. Physiol. Rev. 89, 147–191.
Ley, R.E., Bäckhed, F., Turnbaugh, P., Lozupone, C.A., Knight, R.D., Gordon, J.I., 2005. Obesity alters gut microbial ecology. Proc. Natl. Acad. Sci. U. S. A. 102, 11070–11075.
Lord, R.S., Bralley, J.A., 2008. Clinical applications of urinary organic acids. Part 2. Dysbiosis markers. Altern. Med. Rev. 13, 292–306.
Maslowski, K.M., Vieira, A.T., Ng, A., Kranich, J., Sierro, F., Yu, D., Schilter, H.C., Rolph, M.S., Mackay, F., Artis, D., Xavier, R.J., Teixeira, M.M., Mackay, C.R., 2009. Regulation of inflammatory responses by gut microbiota and chemoattractant receptor GPR43. Nature 461, 1282–U1119.
Musso, G., Gambino, R., Cassader, M., 2010. Gut microbiota as a regulator of energy homeostasis and ectopic fat deposition: mechanisms and implications for metabolic disorders. Curr. Opin. Lipidol. 21, 76–83.
Nguyen, T.L.A., Vieira-Silva, S., Liston, A., Raes, J., 2015. How informative is the mouse for human gut microbiota research? Dis. Model. Mech. 8, 1–16.
Nicholson, J.K., Holmes, E., Kinross, J., Burcelin, R., Gibson, G., Jia, W., Pettersson, S., 2012. Host-gut microbiota metabolic interactions. Science 336, 1262–1267.
Ogata, Y., Nishi, M., Nakayama, H., Kuwahara, T., Ohnishi, Y., Tashiro, S., 2003. Role of bile in intestinal barrier function and its inhibitory effect on bacterial translocation in obstructive jaundice in rats. J. Surg. Res. 115, 18–23.
Ott, S.J., Schreiber, S., 2006. Reduced microbial diversity in inflammatory bowel diseases. Gut 55, 1207–1207.
Rosenfeld, Y., Shai, Y., 2006. Lipopolysaccharide (Endotoxin)-host defense antibacterial peptides interactions: role in bacterial resistance and prevention of sepsis. Biochim. Biophys. Acta Biomembr. 1758, 1513–1522.
Robertson, D.G., Watkins, P.B., Reily, M.D., 2011. Metabolomics in toxicology: preclinical and clinical applications. Toxicol. Sci. 120, S146–S170.
Scheppach, W., 1994. Effects of short-chain fatty-acids on gut morphology and function. Gut 35, S35–S38.
Snedeker, S.M., Hay, A.G., 2012. Do interactions between gut ecology and environmental chemicals contribute to obesity and diabetes? Environ. Health Perspect. 120, 332–339.
Sommer, F., Backhed, F., 2013. The gut microbiota - masters of host development and physiology. Nat. Rev. Microbiol. 11, 227–238.
Sun, X.C., Shao, Y.Y., Jin, Y., Huai, J.P., Zhou, Q., Huang, Z.M., Wu, J.S., 2013. Melatonin reduces bacterial translocation by preventing damage to the intestinal mucosa in an experimental severe acute pancreatitis rat model. Exp. Ther. Med. 6, 1343–1349.
Tirelli, V., Catone, T., Turco, L., Di Consiglio, E., Testai, E., De Angelis, I., 2007. Effects of the pesticide clorpyrifos on an in vitro model of intestinal barrier. Toxicol. Vitro 21, 308–313.
Tremaroli, V., Backhed, F., 2012. Functional interactions between the gut microbiota and host metabolism. Nature 489, 242–249.
Turnbaugh, P.J., Ley, R.E., Mahowald, M.A., Magrini, V., Mardis, E.R., Gordon, J.I., 2006. An obesity-associated gut microbiome with increased capacity for energy harvest. Nature 444, 1027–1031.
Walker, A.W., Sanderson, J.D., Churcher, C., Parkes, G.C., Hudspith, B.N., Rayment, N., Brostoff, J., Parkhill, J., Dougan, G., Petrovska, L., 2011. High-throughput clone library analysis of the mucosa-associated microbiota reveals dysbiosis and differences between inflamed and non-inflamed regions of the intestine in inflammatory bowel disease. BMC Microbiol. 11, 7.
Wang, H.-P., Liang, Y.-J., Long, D.-X., Chen, J.-X., Hou, W.-Y., Wu, Y.-J., 2009. Metabolic profiles of serum from rats after subchronic exposure to chlorpyrifos and carbaryl. Chem. Res. Toxicol. 22, 1026–1033.
Wong, J.M.W., de Souza, R., Kendall, C.W.C., Emam, A., Jenkins, D.J.A., 2006. Colonic health: fermentation and short chain fatty acids. J. Clin. Gastroenterol. 40, 235–243.
Xia, X., Zheng, D., Zhong, H., Qin, B., Gurr, G.M., Vasseur, L., Lin, H., Bai, J., He, W., You, M., 2013. DNA sequencing reveals the midgut microbiota of diamondback moth, *Plutella xylostella* (L.) and a possible relationship with insecticide resistance. PLoS One 8, e68852.
Xu, M.-Y., Sun, Y.-J., Wang, P., Xu, H.-Y., Chen, L.-P., Zhu, L., Wu, Y.-J., 2015. Metabolomics analysis and biomarker identification for brains of rats exposed subchronically to the mixtures of low-dose cadmium and chlorpyrifos. Chem. Res. Toxicol. 28, 1216–1223.
Zhang, Y., Zhang, X.X., Wu, B., Cheng, S.P., 2012. Evaluating the transcriptomic and metabolic profile of mice exposed to source drinking water. Environ. Sci. Technol. 46, 78–83.
Zhang, Y., Zhao, F., Deng, Y., Zhao, Y., Ren, H., 2015. Metagenomic and metabolomic analysis of the toxic effects of trichloroacetamide-induced gut microbiome and urine metabolome perturbations in mice. J. Proteome Res. 14, 1752–1761.
Zheng, X., Xie, G., Zhao, A., Zhao, L., Yao, C., Chiu, N.H.L., Zhou, Z., Bao, Y., Jia, W., Nicholson, J.K., Jia, W., 2011. The footprints of gut microbial-mammalian co-metabolism. J. Proteome Res. 10, 5512–5522.